Pergamon

SCIENCE DIRECT®

Bioorganic & Medicinal Chemistry 11 (2003) 4661–4672

BIOORGANIC & MEDICINAL CHEMISTRY

On How the Conformation of Biliverdins Influences Their Reduction to Bilirubins: A Biological and Molecular Modeling Study

María E. Mora,[a] Sara E. Bari,[b] Josefina Awruch[a] and José M. Delfino[b,*]

[a]*Departamento de Química Orgánica, Facultad de Farmacia y Bioquímica, Universidad de Buenos Aires, Junín 956, 1113 Buenos Aires, Argentina*

[b]*Departamento de Química Biológica, Facultad de Farmacia y Bioquímica, Universidad de Buenos Aires, Junín 956, 1113 Buenos Aires, Argentina*

Received 2 November 2002; accepted 9 June 2003

Abstract—The cyclic 2,18-bridged biliverdin (**2**) is excreted in rat bile without reduction to the corresponding bilirubin. Conformational analysis, employing an optimized Monte Carlo method and a mixed Monte Carlo/stochastic dynamics, reveals that biliverdin IXα (**1**) and the cyclic analogue **2** adopt 'lock washer' conformations, stabilized by the presence of intramolecular hydrogen bonds between $N_{23}...H_{22}N$ and, to a lesser extent, between $N_{23}...H_{24}N$. Although **2** is very similar in overall shape to **1**, the former adopts a 'locked lock washer' conformation unable to undergo fluctuations, thus possibly hampering a proper recognition by biliverdin reductase.

Introduction

Heme catabolism in mammals starts with the enzymatic oxidation of heme to biliverdin IXα which is in turn reduced by cytosolic biliverdin reductase (BVR) to bilirubin IXα.[1,2] However, heme cleavage at other positions has been shown by the presence of isomers of bilirubin IXα under both physiological and pathological conditions in vivo[3–6] or in isolated perfused rat liver.[7] On the other hand, an increased excretion of biliverdin IXβ into rabbit urine has been observed following the administration of hemoglobin or phenylhydrazine as homolytic agent,[8] as well as in urinary samples of healthy adults.[9]

Although the substrate of BVR in mammals is usually biliverdin IXα, this enzyme is unusual in that it has a very broad substrate specificity. Studies performed in vitro and in vivo have demonstrated that BVR readily reduces not only the four biliverdin isomers (α, β, γ, and δ), but also a large number of bilitrienes substituted with polar or nonpolar side chains, as long as they carry two propionate residues.[10,11] Bridged biliverdins of type IXδ were efficiently reduced in vitro,[12] as well as a conformational isomer of biliverdin IXα such as the bridged neobiliverdin IXβ which was also a good BVR substrate in vivo.[13]

In this study, we chose a cyclic analogue of biliverdin IXα for probing conformational features relevant for reduction to bilirubin. In this regard, this analogue had been demonstrated to act as a very poor substrate of BVR in vitro.[14] Here, the hepatobiliary excretion of this pigment was investigated and compared with that of biliverdin IXα. Molecular mechanics simulations allowed us to establish the conformation of **2** by comparison with **1**. Results from our theoretical calculations are discussed in connection with experimental data for the in vivo excretion of these pigments.

Results

Chemistry

We chose to study the cyclic analogue **2** (see Scheme 1) by comparison with biliverdin IXα(**1**). The rationale for this is the following: (i) unlike **1** the covalently linked

*Corresponding author. Tel.: +54-11-4962-5506 or +54-11-4964-8289-9091x116; fax: +54-11-4962-5457; e-mail: rtdelfin@criba.uba.ar or delfino@qb.ffyb.uba.ar

0968-0896/$ - see front matter © 2003 Elsevier Ltd. All rights reserved.
doi:10.1016/S0968-0896(03)00479-6

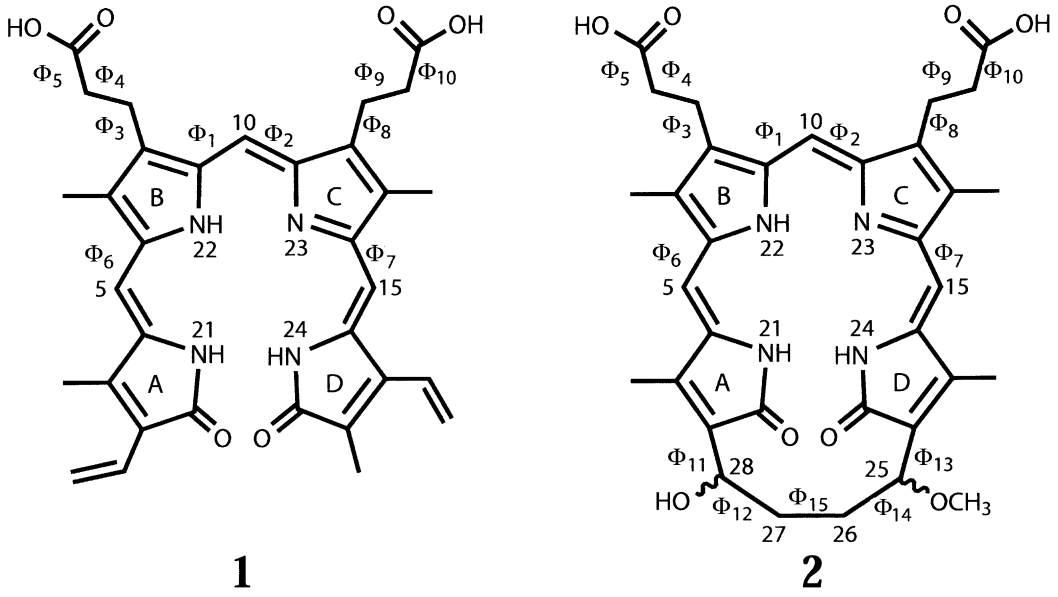

Scheme 1.

A–D cyclic analogue will be unable to stretch; (ii) in order to avoid distorting the overall biliverdin conformation, the design of the bridge includes a flexible four-carbon chain. On the other hand, the choice of a saturated chain does not alter the electronic distribution on the tetrapyrrolic ring system. Thus, **2** appears as an interesting test molecule to be compared with the linear natural form **1**.

Biliverdins **1** and **2** herein employed were synthesized as follows. The dimethyl ester of **1** was obtained from protohemin IX using the coupled oxidation method.[15] Saponification of this dimethyl ester to yield biliverdin **1** was performed similarly to described elsewhere[16] and structure determination of the diacid form was established as reported (see Experimental). The cyclic dimethyl ester of biliverdin **2** was synthesized as described.[17] This compound comprises a mixture of two racemic diastereoisomers which rapidly interconvert at room temperature. The diacid was prepared as described below (see Experimental).

Biological assays in vivo

To test their excretion in bile, compounds **1** and **2** were injected in the bloodstream of male Wistar rats. A qualitative difference is readily apparent: the analysis by TLC of bile components showed that **1** (Fig. 1, panels a, c, e, and g) is efficiently metabolized into bilirubin and its glucuronides, whereas pigment **2** (Fig. 1, panel b) does not give rise to derivatives. No trace of cyclic bilirubin or its conjugates was observed.

The time course observed for the excretion of **1** indicated that its concentration in bile reaches a maximum before 30 min after injection, and that this compound disappears after 90 min (Fig. 1, panel a). Correspond-

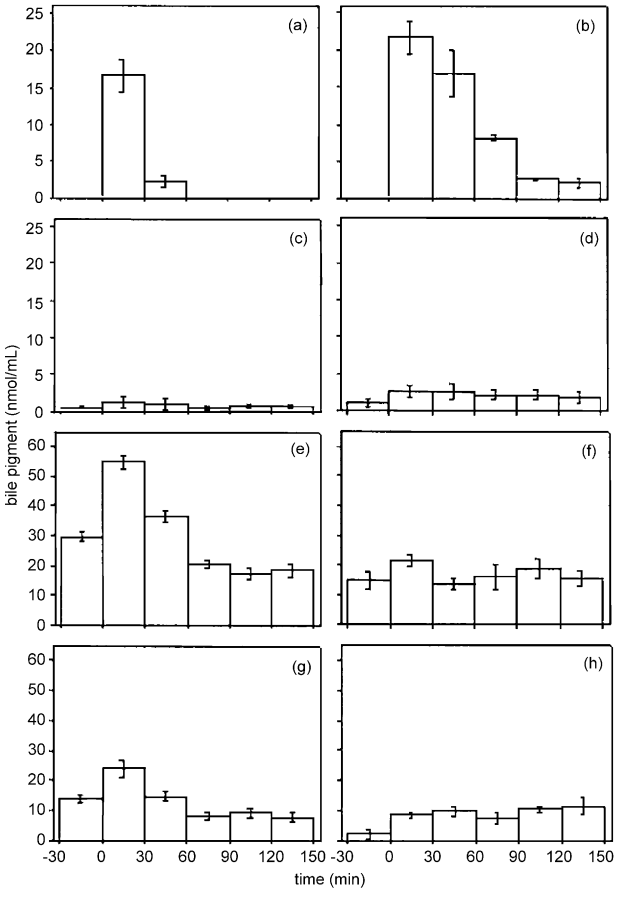

Figure 1. In vivo clearance of bile pigments. The time course of excretion of biliverdins **1** and **2** is shown in panels a and b, respectively. The concentrations of bilirubin IXα (panels c and d) and its glucuronides (the monoglucuronide in panels e and f, and the diglucuronide in panels g and h) are shown below. Data represent the mean value ± standard error of four independent experiments. After injection of these biliverdins no significant variation in the bile flow was observed. For details, see Experimental.

ingly, the concentrations of free bilirubin IXα and its glucuronides also reach a maximum before 30 min and their levels are back to normal after 90 min (Fig. 1, panels c, e and g).

By comparison, the clearance from bile of compound **2** (Fig. 1, panel b) is greatly delayed, namely, this biliverdin does not disappear from bile even at the longest time point assayed (150 min). At all time points tested, no significant difference was seen in the relative proportion of conjugated versus unconjugated forms of endogenous bilirubin, regardless of whether **2** was injected or not (Fig. 1, panels d, f, and h). This result means that the clearance system of bile pigments is not affected by the load of the analogue.

Conformational analysis

Optimized Monte Carlo search and energy minimization of biliverdins. Molecular models of compounds **1** and **2** were initially constructed using the model-building facility implemented in MacroModel.[18] Coordinates for these structures were used as input for BatchMin, the calculation module of this program. In the case of cyclic compound **2** both diastereomeric pairs of enantiomers were considered for the ensuing analysis (see Scheme 1). Nevertheless, the conformational issues presented below hardly depend on the relative configuration of each chiral center.

In order to search the conformational space available to these compounds, we ran an optimized Monte Carlo protocol[19] which allowed free rotation around dihedral angles Φ_i (Scheme 1), which constitute the major determinants of the structure, that is we considered all single bonds along the tetrapyrrole backbone, in addition to the central double bond, and those single bonds belonging to the propionic chains. For compound **2**, the MC method included a ring closure command which defines the single bond connecting the two central methylene groups of the bridge.

Eight planar structures were chosen as starting geometries for biliverdin **1**, that is the Φ_1,Φ_6,Φ_7 torsions adopting the following values: 0, 0, 0; 0, 0, 180; 0, 180, 180; 180, 180, 180; 180, 180, 0; 180, 0, 0; 180, 0, 180; 0, 180, 0°. The central double bond was set to the configuration shown in Scheme 1 ($\Phi = 0$). In the case of cyclic biliverdin **2**, after building the ring closure, reasonably energy minimized structures were chosen as starting geometries. The dihedral angles along the propionic acid chains were initially set to an all anti conformation and the remainder were as shown in Scheme 1.

After this analysis, structures corresponding to the energy minima (as calculated with the force field MM2*, implemented in MacroModel) falling within a 20 kJ/mol window above the global minimum are shown in Table 1a and b. In all cases, regardless of the choice of the initial structure, this search yielded the same set of conformers.

In the case of biliverdin **1**, three distinct non-enantiomeric conformers were found (Table 1a). The global minimum structure of this compound ($\mathbf{1_1}$) adopts a typical helical ('lock-washer') conformation characterized by the presence of two intramolecular hydrogen bonds in the tetrapyrrole backbone, namely, a network exists where N_{23} from ring C acts as a common acceptor

Table 1. Conformations corresponding to energy minima for biliverdin (a) **1**[a] and (b) **2**[a]

a.

Conformer[a]	$\mathbf{1_1}$	$\mathbf{1_2}$	$\mathbf{1_3}$
Dihedral angle (°)[b]			
Φ_1	8.2	0.8	−37.6
Φ_2	2.6	−1.6	−3.0
Φ_3	−94.8	95.3	−107.1
Φ_4	76.6	−78.9	42.4
Φ_5	−89.3	90.8	57.0
Φ_6	−32.0	−30.4	43.4
Φ_7	−36.8	−31.3	−38.6
Φ_8	86.7	−90.7	89.9
Φ_9	−73.8	71.2	−53.0
Φ_{10}	−90.6	93.7	−85.7
Distance (Å)[b]			
$CO^3_8\ldots H^5_{12}O$	1.810	1.804	1.787
$CO^3_{12}\ldots H^5_8O$	1.772	1.770	>3.0
$N_{23}\ldots H_{22}N$	2.187	2.152	2.463
$N_{23}\ldots H_{24}N$	2.430	2.397	2.247
$CO^3_8\ldots H_{24}N$	>3.0	>3.0	2.391
$C_{19}O\ldots H^5_8O$	>3.0	>3.0	1.783
Energy[c] (kJ/mol)	0.00	0.10	6.98

b.

Conformer[a]	$\mathbf{2_1}$	$\mathbf{2_2}$	$\mathbf{2_3}$	$\mathbf{2_4}$	$\mathbf{2_5}$
Dihedral angle (°)[b]					
Φ_1	5.5	−0.5	7.4	1.4	−0.4
Φ_2	1.9	−2.6	2.4	−1.9	1.9
Φ_3	−93.2	94.4	−93.7	94.8	−93.0
Φ_4	76.6	−77.3	76.3	−78.4	77.8
Φ_5	−91.1	91.8	−90.4	91.6	−93.1
Φ_6	−34.6	−33.8	−33.0	−31.7	−36.0
Φ_7	−41.4	−36.2	−40.6	−35.2	−31.9
Φ_8	86.4	−89.1	86.1	−90.4	89.0
Φ_9	−72.0	70.9	−73.0	70.5	−69.9
Φ_{10}	−90.0	91.7	−89.8	93.1	−91.5
Φ_{11}	67.8	68.6	85.5	86.6	56.9
Φ_{12}	65.7	66.2	−86.7	−86.1	90.9
Φ_{13}	74.7	74.4	97.1	97.2	137.7
Φ_{14}	68.7	68.5	−88.9	−89.7	−44.4
Φ_{15}	−148.4	−149.0	133.4	133.3	−63.1
Distance (Å)[b]					
$CO^3_8\ldots H^5_{12}O$	1.807	1.803	1.809	1.803	1.801
$CO^3_{12}\ldots H^5_8O$	1.773	1.771	1.773	1.771	1.772
$N_{23}\ldots H_{22}N$	2.112	2.092	2.138	2.113	2.066
$N_{23}\ldots H_{24}N$	2.408	2.369	2.466	2.427	2.317
Energy[c] (kJ/mol)	0.00	0.56	10.26	11.38	16.52

[a]All minima within a 20 kJ/mol window above the global minimum are reported here. After visual inspection of each structure, only non-superimposable and non-enantiomeric conformers are described.
[b]The definition of dihedral angles follows the convention: Φ_1: $N_{22}C_9C_{10}C_{11}$; Φ_2: $N_{23}C_{11}C_{10}C_9$; Φ_3: $C_9C_8C^1_8C^2_8$; Φ_4: $C_8C^1_8C^2_8C^3_8$; Φ_5: $C^1_8C^2_8C^3_8O^5_8$; Φ_6: $N_{22}C_6C_5C_4$; Φ_7: $N_{23}C_{14}C_{15}C_{16}$; Φ_8: $C_{11}C_{12}C^1_{12}C^2_{12}$; Φ_9: $C_{12}C^1_{12}C^2_{12}C^3_{12}$; Φ_{10}: $C^1_{12}C^2_{12}C^3_{12}O^3_{12}$; Φ_{11}: $C_1C_2C_{28}C_{27}$; Φ_{12}: $C_2C_{28}C_{27}C_{26}$; Φ_{13}: $C_{19}C_{18}C_{25}C_{26}$; Φ_{14}: $C_{18}C_{25}C_{26}C_{27}$; Φ_{15}: $C_{25}C_{26}C_{27}C_{28}$ (see Scheme 1). Values represent dihedral angles and bond distances obtained after the MC optimized method (see Experimental) employing the MM2* force field.
[c]Energy values calculated after molecular mechanics (MM2*) are reported as differences with respect to the global minimum.

to H_{22} from ring B and H_{24} from ring D. In addition, the carboxylates of the propionic chains are capable of closing two ancillary hydrogen bonds with each other. Conformers $\mathbf{1_1}$ and $\mathbf{1_2}$ (Fig. 2) show the same helical conformation, where the lactamic carbonyl groups 'pile up' in an opposing orientation, thus maximizing stability by optimization of the inter-ring distance for favorable van der Waals contacts and carbonyl dipole–dipole interaction. Consequently, pyrromethenone rings A and D lie in parallel planes. Conformers $\mathbf{1_1}$ and $\mathbf{1_2}$ differ only in the arrangement adopted by the loop closed by the propionic chains, which lies above or below the B–C ring plane.

By contrast, the higher energy conformer $\mathbf{1_3}$ shows instead an 'edge-to-face' aromatic interaction between the pyrromethenone rings. A characteristic feature of this last structure is the presence of a 'bilirubin-like' hydrogen bond network involving the carboxylate of the propionic chain in position 8 and the amide system of the opposite pyrromethenone (ring D). Note that the oxygen atom of CO_8^3 also serves as acceptor of a hydrogen donated by the carboxylate of the other propionic substituent in C_{12}, thus a partial link still persists between both acidic groups. The distortion from a typical 'lock washer' conformation observed for $\mathbf{1_3}$ becomes evident in the anomalous values for Φ_1 and Φ_6 (Table 1a). Due to its energy, this conformer is expected to contribute little to the overall population. Thus, as will be seen later, the average conformation resembles mostly the geometry of conformers $\mathbf{1_1}$ and $\mathbf{1_2}$ (Table 3).

The conformational search of biliverdin **2** yields five non-enantiomeric low energy conformers (Table 1b and Fig. 2). Conformers $\mathbf{2_1}$ and $\mathbf{2_2}$ adopt identical helical conformations of the bilatriene moiety, differing only in the location—above or below the B–C plane—of the intercarboxylate bridge. The conformation of the substituted butylene bridge for this pair is identical (Φ_{12}, Φ_{14}, Φ_{15}: *gauche* +, *gauche* +, quasi *anti*, respectively, see Table 1b), orienting the central ethylene group almost perpendicularly to the B–C plane. In this conformation the bridge hardly imposes any strain on the overall shape of the helical tetrapyrrole, as ascertained by the very good superimposition with the structures of acyclic biliverdin IXα (conformers $\mathbf{1_1}$ and $\mathbf{1_2}$, Table 2). Thus, stacking interaction between the pyrromethenones (rings A and D) is close to optimal.

Conformers $\mathbf{2_3}$ and $\mathbf{2_4}$ also constitute a pair which show identical tetrapyrrole backbones (and not different from those shown by $\mathbf{2_1}$ and $\mathbf{2_2}$, Table 2), differing at the orientation—above or below the B–C plane—of the interpropionic bridge. By contrast, here the butylene bridge of both structures (Φ_{12}, Φ_{14}, Φ_{15}: quasi *gauche* −, quasi *gauche* −, quasi eclipsed, respectively, see Table 1b) orients the central ethylene moiety roughly parallel to the B-C plane. Localized strain at the level of the bridge is most likely responsible for the approx. 10 kJ/mol difference in energy of the $\mathbf{2_3}$/$\mathbf{2_4}$ pair with respect to the $\mathbf{2_1}$/$\mathbf{2_2}$ pair. This characteristic becomes even more remarkable in the case of conformer $\mathbf{2_5}$ where the bridge shows a more distorted trace (Φ_{12}, Φ_{14}, Φ_{15}: quasi *gauche* +, quasi *gauche* −, *gauche* −, respectively, see Table 1b). In a fashion similar to **1**, all conformers of **2** adopt 'lock-washer' conformations stabilized by backbone hydrogen bonds $N_{23}\ldots H_{22}N$ and $N_{23}\ldots H_{24}N$.

Table 2 summarizes data which facilitates the comparison among conformers of compounds **1** and **2**, including the crystalline structures of biliverdin IXα dimethyl ester[20] and a 2,18-propylene bridged analogue.[21]

With the exception of the highest energy conformers, that is, structure $\mathbf{1_3}$ and to a lesser extent structure $\mathbf{2_5}$, a reasonably good superimposition exists between all calculated conformers and the crystalline dimethylester of **1**. In the latter, rings B and C are slightly off from perfect coplanarity to optimize van der Waals contact between methyl propionates. The bridge in **2** causes the pyrromethenone rings A and D to come closer together than in the crystalline form of the dimethylester of **1**: as a reference, the nitrogen atoms of these rings are displaced inward by 0.7–0.8 Å for conformers $\mathbf{2_1}$/$\mathbf{2_2}$, and by 0.4–0.5 Å for the pair $\mathbf{2_3}$/$\mathbf{2_4}$. These results highlight the remarkable similarity between the conformations adopted by **1** and **2**, that is, in spite of the absence of a covalent closure in biliverdin **1** this molecule adopts a very similar 'lock washer' conformation. Not surprisingly, the shape of the lowest energy conformers of **2** matches closely that adopted by the crystalline 2,18-propylene bridged analogue of biliverdin.[21]

Further evidence on the lack of influence exerted by the propionic chains on biliverdin conformation is found by comparing the global energy minimum conformer of 3,7,8,12,13,18-hexamethyl-2,17-divinyl-21*H*,24*H*-biline-1,19-dione with $\mathbf{1_1}$. The RMS deviation value between these structures was 0.163 Å. In addition, crystalline etiobiliverdin IVγ[22] also superimposes well onto structure $\mathbf{1_1}$ (RMS deviation 0.357 Å). Taken together, these observations demonstrate the ancillary role played by the polar propionate side chains upon the general conformation of the tetrapyrrole backbone.

An independent conformational search employing the AMBER* force field instead of MM2* produced a similar set of minimum energy conformers for **1** and **2**. As an example, for compound **1** a rigid body superimposition of the structures corresponding to the global energy minima calculated with each force field yielded an RMS deviation value of 0.189 Å.

Mixed Monte Carlo/stochastic dynamics. The aim of this study was to generate a conformational ensemble from which to derive the average structure for each biliverdin, with emphasis on a more realistic appreciation of the extent of intramolecular hydrogen bonding. Results from this simulation provide an enhanced picture from that obtained after MC and energy minimization. We believe that molecular features derived in this fashion will assist the understanding of the recognition phenomena of biliverdins by BVR. Towards this end, we applied an advanced MC/SD method[23] already tested on monopropionic, dipropionic and bridged analogues of bilirubin IXα.[13,24]

In the course of this simulation—and similarly to the previous MC study—free rotation was allowed around all torsions Φ_i (Scheme 1). Several runs (up to a maximum of 10 ns) following the protocols described below were carried out starting from the global energy minima of each compound (see Table 1a and b). For **2** an MC/SD simulation employing a novel Monte Carlo method, namely, a so-called 'jumping between wells/stochastic dynamics'[25] was executed as implemented in BatchMin 5.5.[18] This procedure has been specially indicated for

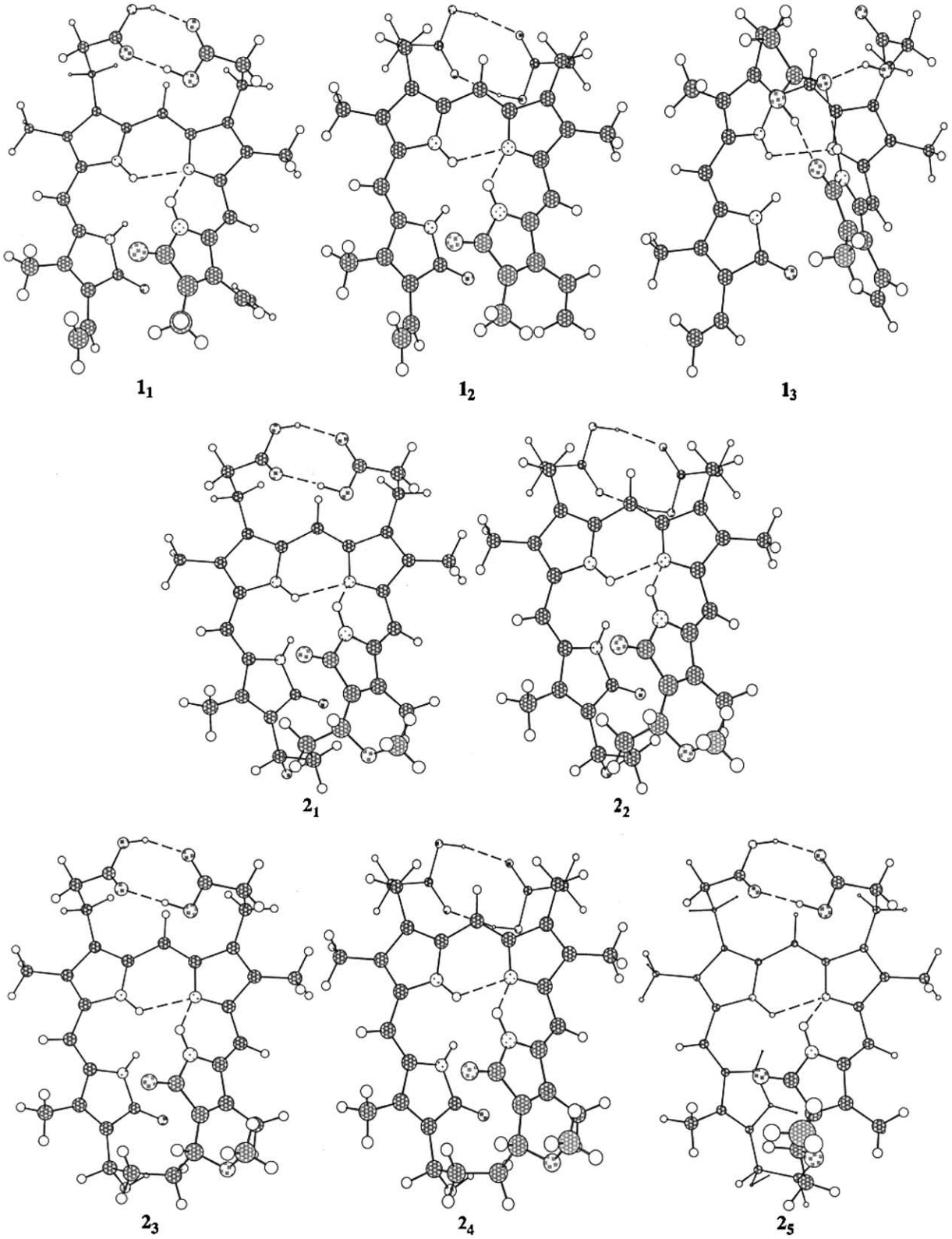

Figure 2. Ball and stick representations of conformers corresponding to energy minima for biliverdins **1** and **2** (see Table 1a and b). Dashed lines represent hydrogen bonds.

Table 2. Comparison of energy minima conformers of biliverdins **1** and **2** and crystalline biliverdin IXα dimethyl ester

	RMS deviation after a rigid body superimposition (Å)[a]							
Conformer	$\mathbf{1_1}$	$\mathbf{1_2}$	$\mathbf{1_3}$	$\mathbf{2_1}$	$\mathbf{2_2}$	$\mathbf{2_3}$	$\mathbf{2_4}$	$\mathbf{2_5}$
$\mathbf{1_1}$	0							
$\mathbf{1_2}$	0.105	0						
$\mathbf{1_3}$	0.852		0					
$\mathbf{2_1}$	0.353			0				
$\mathbf{2_2}$		0.333		0.081	0			
$\mathbf{2_3}$				0.224		0		
$\mathbf{2_4}$					0.221	0.080	0	
$\mathbf{2_5}$				0.240		0.343		0
Crystalline biliverdin IXα dimethyl ester[b]	0.289	0.308	0.866	0.575	0.591	0.393	0.403	0.656
Crystalline 2,18-propylene bridged biliverdin IXα dimethyl ester[c]	0.426	0.364	0.838	0.305	0.279	0.338	0.289	0.211

[a]Only the coordinates of the 25 atoms comprising the tetrapyrrole skeleton (i.e., the tetrapyrrole system without substituents) are compared.
[b]Coordinates taken from the structure of the dimethyl ester of biliverdin IXα (BILVER[20]). The enantiomer had to be considered for the superimpositions.
[c]Coordinates taken from the structure of the dimethyl ester of the 2,18-propylene bridged biliverdin IXα (YAMVIR[21]). The enantiomer had to be considered for the superimpositions.

Table 3. Most frequent dihedral angles for biliverdins **1** and **2** encountered along the MC/SD simulation[a]

Conformer dihedral angle (°)[b]	Chloroform		Water	
	Compd **1**	Compd **2**	Compd **1**	Compd **2**
Φ_1	2.5 (−17.5, 17.5)	−2.5 (−15, 10)	0 (−20, 17)	−2.5 (−17, 10)
Φ_2	0 (−10, 10)	−2.5 (−10, 10)	0 (−10, 10)	−2.5 (−10, 5)
Φ_3	−97.5 (−105, −85)	−95 (−115, −75)	−92.5 (−107.5, −70)	−87 (−122, −47)
Φ_4	75 (60, 85); 180 (−165, 160)[d]	75 (57, 90)[c]; 180 (−162, 162)[c]	62.5 (45, 80)[c]; 180 (−165, 165)[c]	62 (47, 80)[d]; 180 (−162, 162)
Φ_5	−77 (−100, −65)[e]	−92 (−115, −52)	−77.5 (−105, −55)[e]	−90 (−120, −35)
Φ_6	−20 (−35, −5)	−25 (−35, −12)	−20 (−35, 2.5)	−25 (−35, −12)
Φ_7	−17.5 (−35, n.d.)[f];−130 (−147, −115)[d]	−20 (−32, −10)	−15 (−35, n.d.)[f]	−22 (−35, −10)
Φ_8	97 (85, 107)	92 (75, 110)	95 (67.5, 110)	62 (30, 120)
Φ_9	−70 (−87, −55);−177 (−160, 162)[d]	−67 (−82, −52)[c]; 180 (−162, 165)[c]	−60 (−77.5, −45)[c]; 180 (−165, 165)[c]	−62 (−47, −80)[d]; 180 (−162, 162)
Φ_{10}	−80 (−100, −65)[e]	−92 (−117, −62)	−80 (−107.5, −60)[e]	−87 (−122, −40)
Φ_{11}		40 (27, 50)		40 (27, 55)
Φ_{12}		77 (67, 90)		77 (67, 87)
Φ_{13}		40 (27, 55)		42 (30, 57)
Φ_{14}		75 (65, 85)		75 (65, 85)
Φ_{15}		−142 (−150, −135)		−142 (−150, −135)

[a]MC/SD simulations at 300 K in chloroform and in water employing the AMBER* force field were run for 5 ns. This time allows the calculation to converge according to the criteria mentioned in the Experimental.
[b]The definition of dihedral angles follows the convention described in the legend to Table 1. The values represent bond angles for the most populated states (mode), the limits for the width of the distribution bell at half height are reported between parentheses.
[c]Populations of comparable size.
[d]Minor population.
[e]A very minor population exists too, but it is not reported.
[f]Non-determined due to partial overlap.

cyclic compounds and requires as starting geometries the set of conformers found after the Monte Carlo conformational analysis (see Table 1b).

In each case, regardless of the choice of initial structure, average values for torsions and hydrogen bonds parameters calculated on the final conformational ensemble were identical (Table 3). Parallel calculations were performed employing chlorofom and water as solvents. After an initial equilibration period of 50 ps, each simulation was allowed to proceed for up to 5 ns at 300 K. This protocol ensures that the following convergence criteria are met: (i) the final average values for interatomic distances and angles are the same, regardless of the choice of starting structure; (ii) mean temperature and mean enthalpy reach numerical stability; and (iii) a

symmetrical distribution for all freely rotating dihedral angles is observed.

The most frequent values of Φ_i found along the MC/SD run are reported in Table 3. The relative tendency to form hydrogen bonds is described in Table 4a and b for chloroform and water, respectively. On average **1** adopts a 'lock washer' conformation similar to minimum energy structures $\mathbf{1_1}$ and $\mathbf{1_2}$, as evidenced by the close agreement observed between Φ_i values reported in Table 3 with those in Table 1a.

For the simulation in chloroform, the two propionic acid chains alternatively close rings above or below the tetrapyrrolic system, giving rise to opposite gauche conformations (Φ_4, $\Phi_9 \sim \pm 70°$). Ready interconversion between conformers occurs, as evidenced by the symmetrical bimodal distributions found for all Φ_i (note that these two populations collapse whenever the torsion adopts values close to 0° or 180°). Minor populations were also observed which represent rare occurrences where the pyrromethenone ring D flips away ($\Phi_7 \sim \pm 130°$) and/or conformers where propionic acid chains take a more sterically stable extended form (Φ_4, $\Phi_9 \sim 180°$), thus causing the loss of intercarboxylate hydrogen bonds. These results stress that an extended conformation does not appear to be significantly populated.

Remarkably, the average structures of **1** and **2** resemble each other closely, but the covalent bridge in the latter imposes a severe hindrance on the interconversion between 'lock-washers' of opposite helicity. Despite this fact, the bridge does not perturb the almost ideal stacking interaction occurring between rings A and D. As regards the torsional preferences of the propionic side chains in **2**—reflected in the increased allowance of angles Φ_4 and Φ_9 corresponding to the *anti* position—this trend originates in the lesser tendency of this compound to form intercarboxylate hydrogen bonds (Table 4a and b).

The evidence presented in Table 4a shows that **1** and **2** are able to form interpropionic hydrogen bonds in chloroform, although a slightly lower tendency insinuates for the latter. By contrast, in water (Table 4b) the chance of hydrogen bond formation between carboxylates for both compounds is obliterated. Consistent with this, a somewhat wider distribution of torsion angles Φ_3–Φ_5 and Φ_8–Φ_{10} is observed in water. The moderately lower stability of the interpropionic hydrogen bonds observed for compound **2**, as compared to **1**, most likely results from restrictions on conformer interconversion of the tetrapyrrole framework imposed by the substituted butylene bridge ('locked lock-washer').

Remarkably, the tendency to form N...H–N bonds is similar for both biliverdins and does not change at all with the solvent milieu. In this regard, the subtly lower prevalence of the $N_{23}...H_{24}N$ bond, as compared to the $N_{23}...H_{22}N$ bond, might reflect the lesser relative mobility of the central rings. These results are consistent with those of Gorb et al.,[26] who concluded that solvation effects on conformer equilibria are negligible in chloroform and other similarly dipolar and non-polar solvents. Unlike the situation prevailing in bilirubins[13,24,27] no other hydrogen bond appears to be significantly represented in the conformational ensemble (see legend to Table 4a), a likely consequence of the quasi planarity of the conjugated a,b,c-bilitriene system.

Discussion

Detailed experimental and molecular modeling conformational analyses of bile pigments have been the matter of many studies (for an account of these see ref 28). In this paper, we address conformational aspects of biliverdins to aid the understanding of molecular features relevant for the biological reduction to bilirubins. To achieve this goal, we carried out experiments in vivo employing a conformationally constrained analogue of biliverdin IXα (**2**) and completed a comparative conformational analysis of both the acyclic molecule **1** and this bridged analogue **2**.

Results presented herein indicate that **1** and **2** show a very similar 'lock-washer' conformation, as attested by the high level of similarity found for the minimum energy conformers of **1** and **2** (e.g., the RMS deviation between $\mathbf{1_1}$ and $\mathbf{2_1}$ equals 0.353 Å, see Table 2). Moreover a molecular dynamics simulation shows that, on average, both compounds adopt conformations which resemble each other closely and which are dominated by the minimum energy structures. In fact, only minor differences were found in the ability to form interpropionic hydrogen bonds. However, this could hardly be a significant difference in an aqueous solvent, where different counter ions from the solution or from amino acid side chains of BVR can act as partners. We should point out that even though the MC analysis demonstrates that all low energy conformers of both compounds maintain intercarboxylate hydrogen bonds, the subsequent MD analysis proved that this feature is not required to keep the 'lock-washer' conformation of the tetrapyrrole backbone. Indeed, although these bonds form to some extent in chloroform, they break up in water. If so, in the aqueous solvent carboxylates would be free to interact with oppositely charged groups in the protein. This is unlike the situation found for bilirubin IXα where propionates become important to stabilize the 'ridge-tile' conformation.[13,24,27] By contrast, for both compounds dealt with in this paper, the $N_{23}...H_{22}N$ bond, but slightly less so the $N_{23}...H_{24}N$ bond persists in water. No other carboxylate-carbonyl or carboxylate–imine hydrogen bond appears to occur.

One should clearly distinguish between those molecular features relevant for the enzymatic reduction from the intrinsic tendency of these molecules to be reduced with chemical reagents such as sodium borohydride. In this regard, a 4-mM solution of this reagent in methanol converted ca. 55% of biliverdin **1** methyl ester and 40% of biliverdin **2** methyl ester to their corresponding bilirubins in 15 min.[14] Nevertheless, analogue **2**, in its diacid form, fails to act as a substrate of BVR in vitro.[14]

Table 4. Relative tendency to form hydrogen bonds for biliverdins **1** and **2** in (a) chloroform and (b) water

Hydrogen bond[a]	Compound **1**		Compound **2**	
	AMBER*	MM2*	AMBER*	MM2*
a. Chloroform				
CO^{3}_{8}...$H^{5}_{12}O$				
Distance (Å)[b]	1.85 (0.2)	1.85 (0.15)	1.85 (0.2)	2.20 (0.27)
O–H...O angle (°)[b]	147 (20)	147 (21)	150(20), 65 (26)	140 (11)
H...O=C angle (°)[b]	130 (16)	135 (11)	127 (19)	132 (14), 35 (7)
%av (%−, %+)[c]	65 (54, 70)	94 (82, 96)	37 (31, 40)	37(20, 44)
CO^{3}_{12}...$H^{5}_{8}O$				
Distance (Å)[b]	1.85 (0.17)	1.80(0.12)	1.85 (0.2)	1.85 (0.18)
O–H...O angle (°)[b]	147 (20)	150 (16)	150 (20), 67 (21)	150 (15), 115 (15)
H...O=C angle (°)[b]	130 (16)	135 (12)	127 (20)	118 (17)
%av (%−, %+)[c]	61 (50, 66)	84 (77, 86)	34 (29, 37)	62 (47, 82)
N_{23}...$H_{22}N$				
Distance (Å)[b]	2.25 (0.15)	2.25(0.15)	2.15 (0.15)	2.15 (0.15)
N–H...N angle (°)[b]	117 (6)	112 (7)	117 (8)	112 (7)
%av (%−, %+)[c]	93 (50, 99)	89 (40, 99)	99 (80, 100)	97 (66, 100)
N_{23}...$H_{24}N$				
Distance (Å)[b]	2.40 (0.2)	2.45 (0.22)	2.30 (0.2)	2.40 (0.22)
N–H...N angle (°)[b]	115 (6)	107 (7)	112 (7)	105 (7)
%av (%−, %+)[c]	80 (26, 94)	46 (5, 82)	91 (34, 100)	58 (7, 95)
b. Water				
CO^{3}_{8}...$H^{5}_{12}O$				
Distance (Å)[b]	>3.0	>3.0	>3.0	>3.0
O–H...O angle (°)[b]	n.d.	n.d.	n.d.	n.d.
H...O=C angle (°)[b]	n.d.	n.d.	n.d.	n.d.
%av (%−, %+)[c]	5 (4, 6)	2 (1.6, 2.2)	1.5 (1.1, 1.8)	0.5 (0.2, 0.7)
CO^{3}_{12}...$H^{5}_{8}O$				
Distance (Å)[b]	>3.0	>3.0	>3.0	>3.0
O–H...O angle (°)[b]	n.d.	n.d.	n.d.	n.d.
H...O=C angle (°)[b]	n.d.	n.d.	n.d.	n.d.
%av (%−, %+)[c]	5 (3, 6)	0.6 (0.4, 0.7)	0.9 (0.6, 1.1)	0.5 (0.3, 0.6)
N_{23}...$H_{22}N$				
Distance (Å)[b]	2.25 (0.15)	2.25 (0.17)	2.15 (0.15)	2.15 (0.15)
N–H...N angle (°)[b]	117 (6)	112 (7)	118 (8)	113 (8)
%av (%−, %+)[c]	91 (46, 99)	87 (36, 98)	99 (82, 100)	97 (64, 100)
N_{23}...$H_{24}N$				
Distance (Å)[b]	2.30 (0.17)	2.45 (0.20)	2.30 (0.20)	2.45 (0.20)
N–H...N angle (°)[b]	104 (6)	109 (6)	113 (8)	106 (6)
%av (%−, %+)[c]	84 (28, 97)	55 (7, 90)	89 (32, 100)	57 (6, 95)

MC/SD simulations at 300 K in chloroform (a) or water (b) employing the AMBER* force field were run for 5 ns. This time allows the calculation to converge according to the criteria mentioned in the Experimental.

[a]The eventual formation of hydrogen bonds $C_{19}O...H^{5}_{8}O$, $C_1O...H^{5}_{12}O$, $CO^{3}_{8}...H_{24}N$, $CO^{3}_{12}...H_{21}N$, $CO^{3}_{12}...H_{22}N$, $C_1O...H^{5}_{8}O$, $C_{19}O...H^{5}_{12}O$, $OH^{5}_{8}...N_{23}$, $CO^{3}_{8}...H_{21}N$, $CO^{3}_{8}...H_{22}N$, $CO^{3}_{12}...H_{24}N$ was also examined, but they were never observed, that is H...Y distance >5 Å.

[b]The convention for bond distances and angles is stated in the legend to Table 1. These values correspond to the most populated states (mode), the half-width of the distribution bell at half height is reported between parentheses.

[c]Population of H-bonded conformations, as estimated on each conformer found along the run. By definition, the H-bonds C–O...H–O should meet the following criteria: average values (%av) were calculated for an O...H distance <2.5 Å, O...H–O angle >120° and C–O...H angle >90°;%+ values result from a less stringent definition of the H-bond, namely, an O...H distance <2.75 Å, O...H–O angle >108° and C–O...H angle >81°; %−values result from a more stringent definition, namely, an O...H distance <2.25 Å, O...H–O angle >132° and C–O...H angle >99°. For N...H–N hydrogen bonds, %av values were calculated for a N...H distance <2.5 Å, and N...H–N angle >100°; %+ values result from an N...H distance <2.75 Å and N...H–N angle >90°; and%−values result from a N...H distance <2.25 Å and N...H–N angle >110°.

Another example of a bridged molecule is N_{21},N_{24}-methano-mesobiliverdin XIIIα dimethyl ester, a molecule that is forced to take a 'porphyrin-like' shape and which is efficiently reduced to bilirubin with sodium borohydride.[29] However, results from enzymatic reduction of this biliverdin were not reported. Thus, the A–D closure of the tetrapyrrole ring by itself does not appear to pose an impediment on the chemical reduction process.

The chemical evidence points out the lesser importance that electronic factors might have to explain differences in the trend shown by these compounds to be reduced enzymatically. Therefore, the focus should rather be put on eventual conformational differences and/or on other characteristics—such as overall flexibility, amphipaticity or goodness of fit—important for the molecular recognition phenomenon of the substrate by the enzyme.

Our results should be discussed in the context of the recently elucidated structures of BVRs: biliverdin IXα reductase from rat liver (BVR-A)[30] and biliverdin IXβ reductase from human origin (BVR-B).[31] These structures highlight the importance of a correct positioning of the tetrapyrrole substrates for catalysis to proceed efficiently. In the case of BVR-B, a non-productive complex with biliverdin IXα was obtained, where steric hindrance appears as the main factor preventing biliverdin IXα from binding productively at the enzyme active site, (i.e., with its C_{10} adequately positioned for direct hydride transfer from the NADPH cofactor). Remarkably, no major distortion of substrate conformation—such as a global stretching of the molecule—is required to accommodate it into the active site. Consistent with this, for **1** our results indicate that a substantial energy barrier should be overcome to linearize the molecule (note the absence of this geometry in Table 1a). In this context, more subtle reasons could be playing a major role to explain why biliverdin **2** is not a substrate of BVR-A. Since in our case the positions for propionates substitution are the same for **1** and **2**, then non-productive binding, if it exists at all, will not be due to the same reasons illustrated in the case of the interaction of biliverdin IXβ with BVR-B. On the other hand, BVR-A is known to be more promiscuous towards substrate recognition, as long as two propionates—regardless of position—are present in the molecule.[10] In the structure of BVR-A, four basic residues were proposed to bind the substrate and Tyr 97 could possibly act as proton donor/acceptor in the reduction process.[30] Unfortunately, there is not yet a complex with substrates or analogues available for this enzyme which could help elucidate this matter further. Our contention is that no major structural rearrangements of the substrate need to take place to allow recognition, in a manner not unlike that observed in BVR-B complexes.[31]

Compounds **1** and **2** differ in the polarity at the edges: while **1** has a single polar end, namely that bearing the propionic chains, **2** includes also polar groups at the oppositely located bridge. In agreement with this, the TLC analysis of these biliverdins shows that **2** is slightly more polar than **1** (see Experimental). Nevertheless these characteristics may bear little influence on the susceptibility to the enzymatic reduction by BVR, since hematobiliverdin IXα bearing two β-hydroxyethyl chains on rings A and D does not pose an impediment for reduction.[10,32] On the other hand, the swapping of methyl and vinyl substituents is also unlikely to make any difference.[10,16,33]

By itself, the presence of the bridge in **2**—including the existence of chiral centers and polar substituents—cannot be ruled out as a factor hampering the correct fitting of this molecule into the active site of the enzyme. Nevertheless, an impediment of this sort is less likely due to the shallow nature of the pocket surrounding both NADPH and biliverdin.[30]

We favor the reduced flexibility exhibited by compound **2**, which is essentially a 'locked lock washer' (see Table 3 and ref 17), as the main reason responsible for its inability to act as substrate. Correct accommodation at the active site of the enzyme will only be possible in a molecule able to undergo conformational fluctuations. In this vein, the requirement for some extent of flexibility of substrate molecules has been argued in the context of the recognition of open chain tetrapyrroles by BVRs.[34]

Experimental

Electronic absorption spectra were determined using a Hitachi U-2000 spectrophotometer. ^{1}H NMR spectra were recorded on Bruker MSL 300 and AM 500 spectrometers. Mass spectra were obtained with TRIO 2-2000 spectrometer in the electronic ionization mode at 70 eV. Melting points were determined on a Kofler melting point apparatus and were not corrected. Bovine albumin (98–99%, w/w) was purchased from Sigma Chemical Co. All other chemicals used were of reagent grade. Solvents were distilled before use.

Synthesis of biliverdins

Biliverdin IXα (1). The coupled oxidation method applied to protohemin IX, followed by cleavage of the verdohaemochrome in potassium hydroxide/methanol and esterification with BF_3/methanol, afforded a mixture of the four isomers of biliverdin IX dimethyl esters.[15] After repeated TLC separations of this mixture on silica gel plates (20×20 cm, silica gel F_{254}; 0.25 mm thick, Riedel de Haën) developed with chloroform/acetone (19:1, v/v), biliverdin IXα dimethyl ester was isolated. The plates were dried at room temperature protected from light, the green band corresponding to the dimethyl ester of 1 was scraped off and eluted with chloroform/methanol (17:3, v/v). The extract was filtered through a sintered glass filter and the solvent was then evaporated at room temperature under high vacuum in the dark. The compound was then recrystallized from dichloromethane and hexanes. The purity of this sample was checked by bidimensional TLC analysis in chloroform/acetone (19:1, v/v, solvent 1) and hexanes/acetone/propionic acid (48:12:4, v/v, solvent 2). ^{1}H NMR, UV–vis, MS and melting point analyses were coincident with those reported in the literature.[15,35]

Saponification of the dimethyl ester of **1** (1 mg) was achieved by dissolving this compound in methanol (2 mL) and aqueous 1 M sodium hydroxide (2 mL). The solution was left to react at 37 °C for 2 h under nitrogen and dim light.[16] At the end, the mixture was neutralized with glacial acetic acid, extracted with dichloromethane, the organic phase was washed with water, and dried by filtration through paper soaked with dry dichloromethane. This solvent was then evaporated under vacuum at room temperature and the solid residue was kept at −20 °C in the dark. A sample of the diacid was run on silica gel TLC, developed with chloroform/methanol/water (48:28:6, v/v; R_f 0.70), to check for the absence of the starting material (diester). In addition, the UV–vis spectrum and the MS analysis

of this material were identical to those reported in the literature.[35,36]

Cyclic 2,18-bridged biliverdin (2). The diester of **2** was synthesized, purified and characterized as described.[17] Saponification of the dimethyl ester of **2** was achieved by dissolving this compound (ca. 0.5 mg) in methanol (3 mL) and aqueous 1 M sodium hydroxide (1.5 mL). This solution was left in the dark under nitrogen overnight at room temperature. The workup procedure was identical to that described before for **1**. The purity of this material was checked by running a sample on a silica gel TLC developed in chloroform/methanol/water (48:28:6, v/v; R_f 0.60). The UV–vis spectrum of this compound in methanol shows bands with maxima at 379 nm ($\varepsilon = 48{,}000\ M^{-1}\ cm^{-1}$) and 662 nm ($\varepsilon = 15{,}800\ M^{-1}\ cm^{-1}$), similar to those reported for the dimethyl ester.[17] The ^1H NMR spectrum taken in $CDCl_3$ shows the absence of OCH_3 groups, by comparison with the precursor (δ 3.69). In addition, an upfield shift (from δ 2.63 to δ 2.32) was observed for the signal corresponding to the CH_2 groups next to CO_2R.

Biological experiments

Animals. Male Wistar rats weighing 300–400 g were obtained from the Animal House of Facultad de Farmacia y Bioquímica, Universidad de Buenos Aires.

Solution of pigments for injection. Compounds **1** (0.1 mg, 172 nmol) and **2** (0.2 mg, 318 nmol) were dissolved in 0.05 mL of 0.1 M sodium hydroxide and 1 mL of albumin solution (10%, w/v, bovine albumin dissolved in 0.15 M sodium chloride solution) was added.[11]

Studies on biliary excretion. The rats were kept under anesthesia with diethylether and the common bile duct was cannulated with 10 cm of PE-10 tubing and protected from light with aluminum foil. The left femoral vein was also cannulated in the same fashion and each biliverdin solution was injected into the animal via the catheter for about 1 min with a 1-mL syringe. Immediately thereafter, a continuous infusion (1 mL/h) of 0.15 M sodium chloride solution containing 5% (w/v) glucose was started and maintained for the length of the experiment.[11,13,24,37]

Throughout the experimental period, room temperature was 20 °C and the body temperature of rats was maintained with infrared lamps. Bile was collected in tubes placed on ice, protected from light and the volume (0.35 ± 0.04 mL per time point) was measured during the common bile duct cannulation ($t = 0$ min) and at 30, 60, 90, 120, and 150 min after injection. These values were corrected for the time taken by bile to flow through the dead volume of the cannula (19 μL).

Extraction from bile and separation of pigments. Biliary excretion of each pigment was studied on four Wistar rats. Bile samples were acidified by the addition of 8 vols of glycine–HCl buffer (pH 1.8) followed by the addition of 2 vols of ascorbic acid solution (100 mg/mL) saturated with sodium chloride.[38] An excess of salt was added to keep the solution saturated before extracting several times at 0–4 °C with chloroform/ethanol (1:1, v/v).[7,11,13,24,32]

The concentrated extract of each animal was then applied to silica gel plates (20×20 cm, silica gel F_{254}, 0.25 mm thick, Riedel de Haën), developed with chloroform/methanol/water (48:28:6, v/v). The plates were dried and the yellow bands of bilirubins were scraped off and eluted from the silica with methanol/water (1:1, v/v). Free bilirubin IXα and its conjugates were quantitated by measuring the absorbance in the range 444–453 nm ($\varepsilon = 60{,}000\ M^{-1}\ cm^{-1}$).[39] The green bands of biliverdins ($R_f = 0.70$ and $R_f = 0.60$ for biliverdins **1** and **2**, respectively) were scraped off and eluted from the silica gel with methanol.

Identification of biliverdins. Methanol–5% H_2SO_4 (1 mL, v/v) was added to the methanolic solution (1 mL) containing each biliverdin and kept at 0–5 °C overnight in the refrigerator. Chloroform (1 mL) was added and the solution washed with water (1 mL), a 10% $NaCO_3H$ solution (1 mL) and, finally, with water (1 mL). At the end, it was dried with Na_2SO_4, filtered and the solvent evaporated under nitrogen. The amount of biliverdin IXα dimethyl ester was estimated by measuring the absorbance in methanol at 374 nm and at 664 nm ($\varepsilon = 50{,}600\ M^{-1}\ cm^{-1}$ and $\varepsilon = 14{,}300\ M^{-1}\ cm^{-1}$, respectively).[7] Cyclic biliverdin dimethyl ester was estimated by measuring the absorbance at 380 and at 660 nm ($\varepsilon = 45{,}500\ M^{-1}\ cm^{-1}$ and $\varepsilon = 15{,}200\ M^{-1}\ cm^{-1}$, respectively). Identification of biliverdin IXα and cyclic biliverdin dimethyl esters was performed using mass spectrometry.

Identification of bilirubins. The free and conjugated bilirubin solutions were evaporated under vacuum at room temperature. The structures of bilirubin IXα, bilirubin IXα monoglucuronide and bilirubin IXα diglucuronide were confirmed by transformation into their corresponding azopigments. Methanolysis of these pigments was followed by the analysis of their methyl esters and conjugated sugars by using established procedures.[3,7,11,13,24,32,38]

Conformational search

Molecular mechanics calculations were carried out with MacroModel 5.5 and BatchMin 5.5[18] running on a SGI O2 workstation (R10000, 320 MB RAM, 54 MB hard disk) under the Irix 6.5 operating system.

Optimized Monte Carlo search, energy minimization and relative stability of isomers. In this paper we used MM2* and AMBER* force fields (the versions of MM2 and AMBER, respectively, as implemented in MacroModel).[40] By default, atomic partial charges are calculated from data in the molecular mechanics force field chosen. Both force fields use distance-dependent dielectric electrostatics. The electrostatic equation used by MM2* uses partial charges and Coulomb's law, instead

of the standard dipole-dipole electrostatics. MM2* includes approximate parameters for hydrogen bonds which were adjusted to mimic AMBER hydrogen bonding potentials. AMBER* is identical to authentic AMBER,[41] with additions. A number of generalized parameters have been added to the field to allow qualitative modeling on many types of molecules. The field is supplied with the united-atom AMBER charge set, and Kollman's 6,12-Lennard Jones hydrogen bonding treatment.[42]

The conformational search of biliverdins was carried out with an optimized Monte Carlo method.[43] Energy minimization used a conjugated gradient method, with a final gradient of 0.01 kcal/Å mol as the criterion for convergence. After the Monte Carlo steps, initial conformers were partially minimized (250 iterations), and the subset of resulting structures were further minimized until convergence. In this process, duplicate and high-energy structures were discarded. In the end, all non-enantiomeric conformers within 20 kJ/mol above the global minimum were tabulated. Atoms belonging to the tetrapyrrole backbone and the propionic acid substituents were taken into account for comparisons. Starting geometries for biliverdins **1** and **2** were as indicated in Results. In all cases, each run included 50,000 Monte Carlo steps, which sufficed to sample the conformational ensemble.

Mixed Monte Carlo/stochastic dynamics. In order to simulate the conformational ensemble of biliverdin **1** we adopted a mixed Monte Carlo/stochastic dynamics (MC/SD) method,[23] which we tested before with bilirubin analogues.[13,24] In the course of the simulation, every SD time step is followed by an MC step. In general, the running time was 6 ns after an initial equilibration time of 50 ps. A time step of 1.5 fs was used for the SD part. In all cases, the MC acceptance ratio was never lower than 0.3% or higher than 5%.

For biliverdin **2** a simulation of the conformational ensemble following the Monte Carlo (jumping between wells)/stochastic dynamics protocol implemented in BatchMin[40] was carried out on the set of torsion angles indicated in Scheme 1. Starting structures for these runs were taken from the output of the Monte Carlo conformational search.

MC/SD simulations were run at 300 K in chlorofom or in water employing the semianalytical solvation treatment GB/SA[43] and the AMBER* or MM2* force field parameters. The default cut-off distance of 12 Å was increased to 50 Å in the electrostatics term. The torsional degrees of freedom were as indicated in Scheme 1. No constraint was put to torsions, and not more than two dihedral angles were allowed to change at each Monte Carlo step.

A hydrogen bond is formed whenever the criteria for bond length and bond angles described in the legend to Table 4a are met. Depending on the stringency of these criteria, the actual calculated percentages vary within narrow limits (Table 4a and b).

Acknowledgements

This work was supported by grants from the Consejo Nacional de Investigaciones Científicas y Técnicas (CONICET), Agencia Nacional para la Promoción de la Ciencia y la Tecnología (ANPCyT) and Universidad de Buenos Aires, Argentina. We thank Dr. Marcelo J. Kogan for suggestions and revision of an early version of this work. The expert technical assistance with animal handling of Mr Alejandro V. Ceccarelli and Ms Cecilia Ricciardelli is appreciated.

References and Notes

1. Schmid, R.; McDonagh, A. F. In *The Porphyrins*; Dolphin D., Ed.; Academic: New York, 1979; Vol. VI, p 257.
2. Frydman, R. B.; Frydman, B. *Acc. Chem. Res.* **1987**, *20*, 250.
3. Blumenthal, S. G.; Taggart, D. B.; Ikeda, R. M.; Ruebner, B. H.; Bergstrom, D. E. *Biochem. J.* **1977**, *167*, 535.
4. Heirwegh, K. P. M.; Van Hees, G. P.; Leroy, P.; Van Roy, F. P.; Jansen, F. H. *Biochem. J.* **1970**, *120*, 877.
5. Gordon, E. R.; Chan, T. H.; Samodai, K.; Goresky, C. A. *Biochem. J.* **1977**, *167*, 1.
6. Yamaguchi, T.; Nakajima, H. *Eur. J. Biochem.* **1995**, *233*, 467.
7. Awruch, J.; Mora, M. E.; Lemberg, A.; Coll, C. T.; Frydman, R. B. *Biol. Chem. Hoppe-Seyler* **1994**, *375*, 617.
8. Hirota, K.; Yamamoto, S.; Itano, H. A. *Biochem. J.* **1985**, *229*, 477.
9. Hirota, K. *Biol. Pharm. Bull.* **1995**, *18*, 481.
10. Frydman, R. B.; Tomaro, M. L.; Rosenfeld, J.; Awruch, J.; Sambrotta, L.; Valasinas, A.; Frydman, B. *Biochim. Biophys. Acta* **1987**, *916*, 500.
11. Mora, M. E.; Bari, S. E.; Awruch, J. *Bioorg. Med. Chem. Lett.* **1997**, *7*, 1249.
12. Frydman, R. B.; Bari, S. E.; Tomaro, M. L.; Frydman, B. *Biochem. Biophys. Res. Commun.* **1990**, *171*, 465.
13. Kogan, M. J.; Mora, M. E.; Bari, S. E.; Iturraspe, J.; Awruch, J.; Delfino, J. M. *Bioorg. Med. Chem.* **1999**, *7*, 1309.
14. Bari, S.; Frydman, R. B.; Grosman, C.; Frydman, B. *Biochem. Biophys. Res. Commun.* **1992**, *188*, 48.
15. Bonnett, R.; McDonagh, A. F. *J. Chem. Soc., Perkin Trans. 1* **1973**, 881.
16. Tomaro, M. L.; Frydman, R. B.; Awruch, J.; Valasinas, A.; Frydman, B.; Pandey, R. K.; Smith, K. M. *Biochim. Biophys. Acta* **1984**, *791*, 350.
17. Krois, D.; Lehner, H. *J. Chem. Soc., Perkin Trans. 1* **1989**, 2179.
18. Mohamadi, F.; Richards, N. G. J.; Guida, W. C.; Liskamp, R.; Lipton, M.; Caufield, C.; Chang, G.; Hendrickson, T.; Still, W. C. *J. Comp. Chem.* **1990**, *11*, 440.
19. Chang, G.; Guida, W. C.; Still, W. C. *J. Am. Chem. Soc.* **1989**, *111*, 4379.
20. Sheldrick, W. S. *J. Chem. Soc., Perkin Trans. 2* **1976**, 1457 Coordinates entry BILVER, Cambridge Structural Database System, Version 5.24, Cambridge Crystallographic Data Centre, Cambridge, UK, April 2003.
21. Sturrock, E. D.; Bull, J. R.; Kirsch, R. E.; Pandey, R. K.; Senge, M. O.; Smith, K. M. *J. Chem. Soc. Chem. Commun.* **1993**, 872. Coordinates entry YAMVIR, Cambridge Structural Database System, Version 5.24, Cambridge Crystallographic Data Centre, Cambridge, UK, April 2003.
22. Wagner, U.; Kratky, C.; Falk, H.; Woss, H. *Monatsch. Chem.* **1991**, *122*, 749. Coordinates entry SUBGOL, Cambridge Structural Database System, Version 5.24, Cambridge Crystallographic Data Centre, Cambridge, UK, April 2003.

23. Guarnieri, F.; Still, W. C. *J. Comp. Chem.* **1994**, *15*, 1302.
24. Kogan, M. J.; Mora, M. E.; Awruch, J.; Delfino, J. M. *Bioorg. Med. Chem.* **1998**, *6*, 151.
25. Senderowitz, H.; Guarnieri, F.; Still, W. C. *J. Am. Chem. Soc.* **1995**, *117*, 8211.
26. Gorb, L.; Korkin, A.; Leszczynski, J; Varnek, A.; Mark, F.; Schaffner, K. *THEOCHEM* **1998**, *425*, 137.
27. Person, R. V.; Peterson, B. R.; Lightner, D. A. *J. Am. Chem. Soc.* **1994**, *116*, 42, and references cited therein.
28. Falk, H. *The Chemistry of Linear Oligopyrroles and Bile Pigments*; Springer: Wien, 1989.
29. Hwang, K.-O.; Lightner, D. A. *Heterocycles* **1994**, *37*, 807.
30. Kikuchi, A.; Park, S.-Y.; Miyatake, H.; Sun, D.; Sato, M.; Yoshida, T.; Shiro, Y. *Nature Struct. Biol.* **2001**, *8*, 221.
31. Barbosa Pereira, P. J.; Macedo-Ribeiro, S.; Párraga, A.; Pérez-Luque, R.; Cunningham, O.; Darcy, K.; Mantle, T. J.; Coll, M. *Nature Struct. Biol.* **2001**, *8*, 215.
32. Awruch, J.; Lemberg, A.; Frydman, R. B.; Frydman, B. *Biochim. Biophys. Acta* **1982**, *714*, 209.
33. Awruch, J.; Tomaro, M. L.; Frydman, R. B.; Frydman, B. *Biochim. Biophys. Acta* **1984**, *787*, 146.
34. Cunningham, O.; Dunne, A.; Sabido, P.; Lightner, D.; Mantle, T. J. *J. Biol. Chem.* **2000**, *275*, 19009.
35. Heirwegh, K. P. M.; Blanckaert, N.; Van Hees, G. *Anal. Biochem.* **1991**, *195*, 273.
36. McDonagh, A. F.; Palma, L. A. *Biochem. J.* **1980**, *189*, 193.
37. Sieg, A.; Stiehl, A.; Heirwegh, K. P. M.; Fevery, J.; Raedsch, R.; Kommerell, B. *Hepatology* **1989**, *10*, 14.
38. Blanckaert, N.; Fevery, J.; Heirwegh, K. P. M.; Compernolle, F. *Biochem. J.* **1977**, *164*, 237.
39. Crawford, J. M.; Ransil, B. J.; Potter, C. S.; Westmoreland, S. V.; Gollan, J. L. *J. Clin. Invest.* **1987**, *79*, 1172.
40. *MacroModel, A Primer*, Version 5.5.; Department of Chemistry: Columbia University, New York, NY 10027, USA, 1996.
41. Weiner, S. J.; Kollman, P. A.; Case, D. A.; Singh, U. C.; Ghio, C.; Alagona, G.; Profeta, S., Jr.; Weiner, P. *J. Am. Chem. Soc.* **1984**, *106*, 765.
42. Ferguson, D. M.; Kollman, P. A. *J. Comp. Chem.* **1990**, *12*, 620.
43. Still, W. C.; Tempczyk, A.; Hawley, R. C.; Hendrickson, T. *J. Am. Chem. Soc.* **1990**, *112*, 6127.